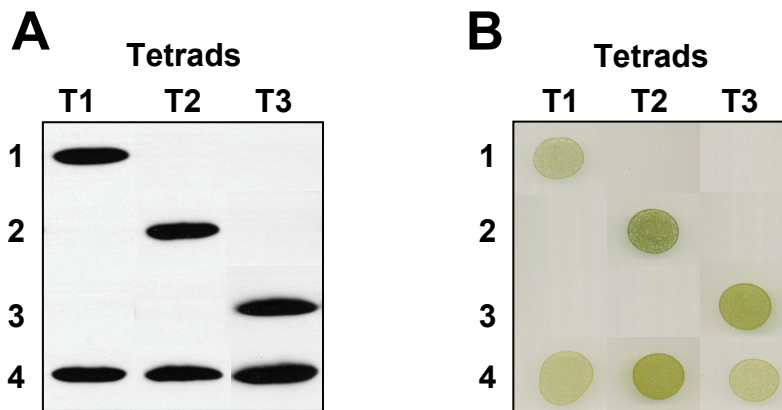


Supplemental Figure 1. Unrooted Phylogenetic Tree of FtsH Proteins.

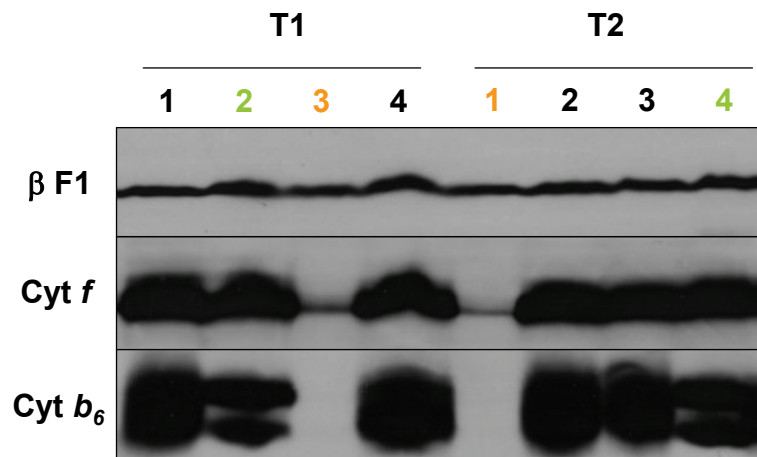
Nuclear encoded FtsH sequences of *Arabidopsis thaliana* (At) and *Chlamydomonas reinhardtii* (Cr) were obtained from Phytosome v9.1 (<http://www.phytosome.net/>), FtsH sequences of *Synechocystis* sp. PCC 6803 (Sy) from cyanobase (<http://genome.microbedb.jp/cyanobase/>), and FtsH sequences of *Escherichia coli* (Ec) and *Saccharomyces cerevisiae* (Sc) from NCBI (<http://www.ncbi.nlm.nih.gov/protein>): At-FtsH1-12, At-FtsHi1 (AT4G23940), At-FtsHi2 (AT3G16290), At-FtsHi3 (AT3G02450), At-FtsHi4 (AT5G64580), At-FtsHi5 (AT3G04340), Cr-FtsH1 (Cre12.g485800), Cr-FtsH2 (Cre17.g720050), Cr-FtsH3 (Cre01.g019850), Cr-FtsH4 (Cre13.g568400), Cr-FtsH7 (g1437), Cr-FtsH11 (g15070), Cr-FHL1 (Cre03.g201100), Cr-FHL2 (Cre09.g393950), Cr-FHL3 (Cre07.g352350), Sy-FtsH1 (slr1390), Sy-FtsH2 (slr0228), Sy-FtsH3 (slr1604), Sy-FtsH4 (slr1463), Ec-FtsH and Sc-YTA10-12. FtsH-like proteins lacking the Zn-binding motif are annotated At-FtsHi and Cr-FHL. 639 sites were retained for the phylogenetic analysis (see Methods and Supplemental Data Set 1). Cr-FHL2 and At-FtsHi3 sequences are shorter of about 200 amino-acids at their C-terminus and miss part of the protease domain. Bootstrap values above 50% are indicated. The scale bar represents the average number of amino-acid changes per site. The major subcellular localizations of eukaryotic FtsHs, in chloroplasts (in green) or mitochondria (in red), are indicated as determined by proteomic and green fluorescent protein studies (in bold) or as predicted (in italics): chloroplast (C), thylakoid membrane (T) with subunit type (A or B), envelope (E), and mitochondrion (M).



Supplemental Figure 2. Back-Cross of *Rccb2-306* mt⁻ with *ccb2* mt⁺ Yields only Parental Ditype Tetrads Showing that the Suppressor Mutation is Monogenic and Nuclear.

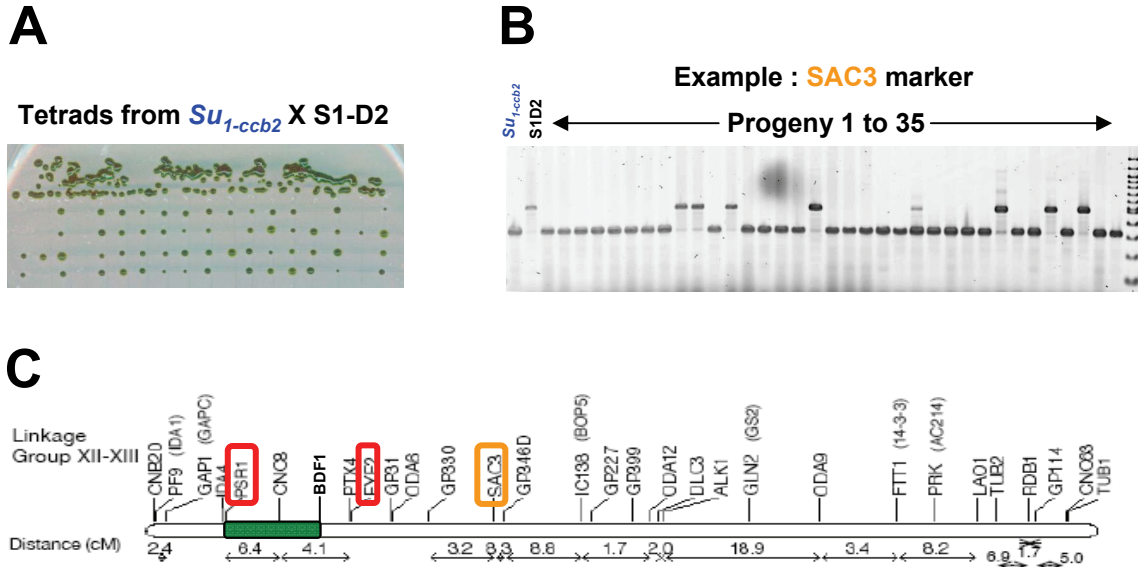
(A) Mendelian segregation of *b₆f* complex accumulation as monitored by immunodetection of subunit IV shown here for three tetrads (T).

(B) Phototrophic growth on minimum media segregates as *b₆f* accumulation.



Supplemental Figure 3. Back-Cross of *Su*_{1-ccb2} with *ccb2* confirms the suppressor effect.

Total cell proteins of two tetratype tetrads (T) grown on acetate medium at $6 \mu\text{E m}^{-2} \text{s}^{-1}$ were separated by SDS/urea-PAGE and the segregation of cytochrome *b*₆*f* complex accumulation is monitored by immunodetection of cytochrome *f* (Cyt *f*) and cytochrome *b*₆ (Cyt *b*₆) using ATP synthase β subunit (β F1) as loading control. *Su*_{1-ccb2} *ccb2* progeny (in green) has a wild-type accumulation of *b*₆*f* subunits with cytochrome *b*₆ lacking covalent heme *c*_i while *ccb2* progeny (in orange) accumulates very low amounts of *b*₆*f* subunits. When cytochrome *b*₆ contains covalent heme *c*_i, it shows up as a diffuse band; when it lacks covalent heme *c*_i, it shows up as a doublet band under these SDS/urea-PAGE conditions. This correlation is demonstrated in Figure 1B by showing immunoblot of cytochrome *b*₆ together with the heme peroxidasic activity assay using tetramethylbenzamidine.

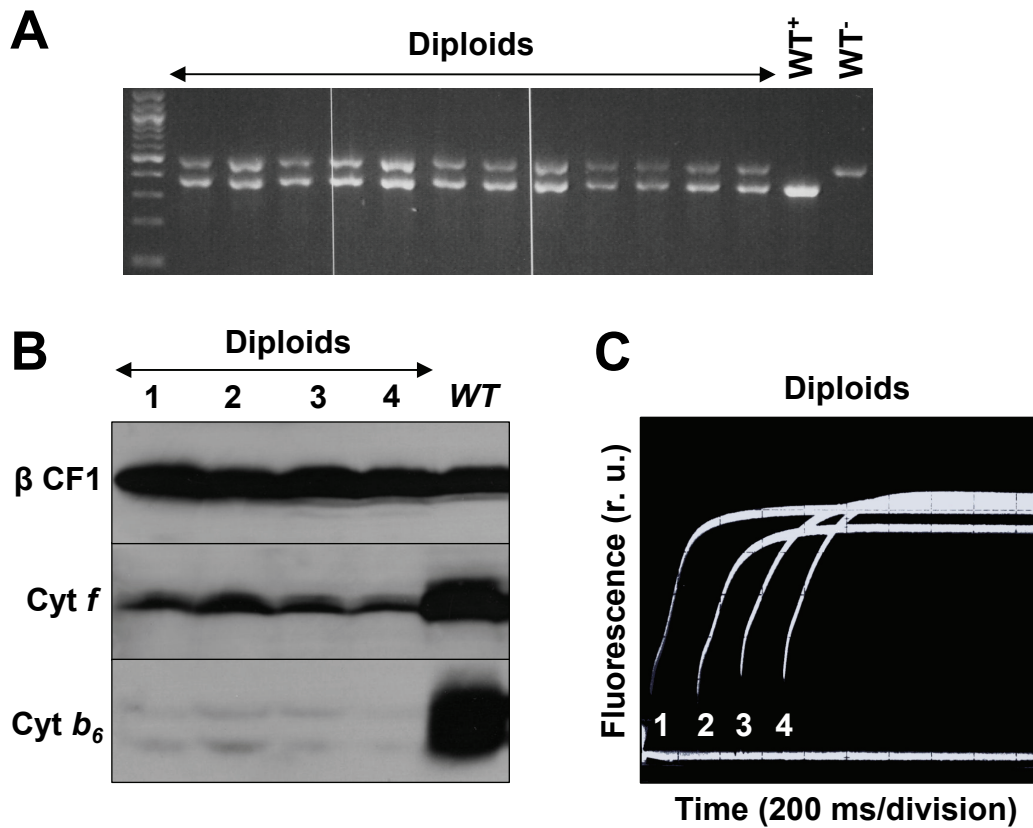


Supplemental Figure 4. Map-Based Cloning of the Suppressor.

(A) Tetrads from the cross of *Chlamydomonas reinhardtii* *Su*_{1-ccb2} with the interfertile *Chlamydomonas grossii* species S1-D2.

(B) Linkage analysis of *Su*_{1-ccb2} mutation to SAC3 marker by PCR; the primers used in a single PCR reaction generate products that differ in size for the *reinhardtii* or *grossii* allele.

(C) *Chlamydomonas reinhardtii* linkage group XII-XIII depicted as a long horizontal rod with known genetic distances between markers (cM) shown by two-headed arrows as published in (Merchant, S. et al. (2007) Science 318: 245-250). The suppressor mutation *Su*_{1-ccb2} was localized in the vicinity of the PSR1 and BDF1 markers.

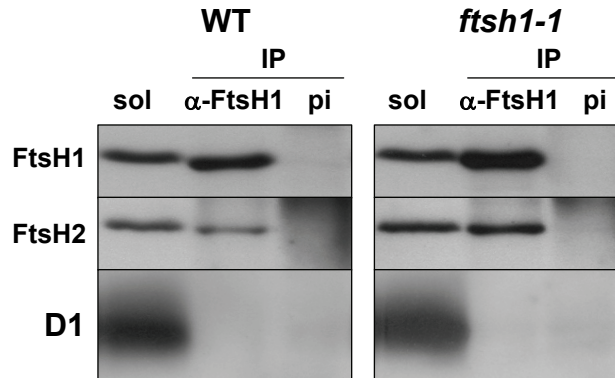


Supplemental Figure 5. Mutation *ftsh1-1* is Recessive in Vegetative Diploids.

(A) PCR mating type test confirms the presence of both mating types in vegetative diploids growing in absence of arginine from cross of *ftsh1-1 ccb2 arg7* with *FTSH1 ccb2 arg2*.

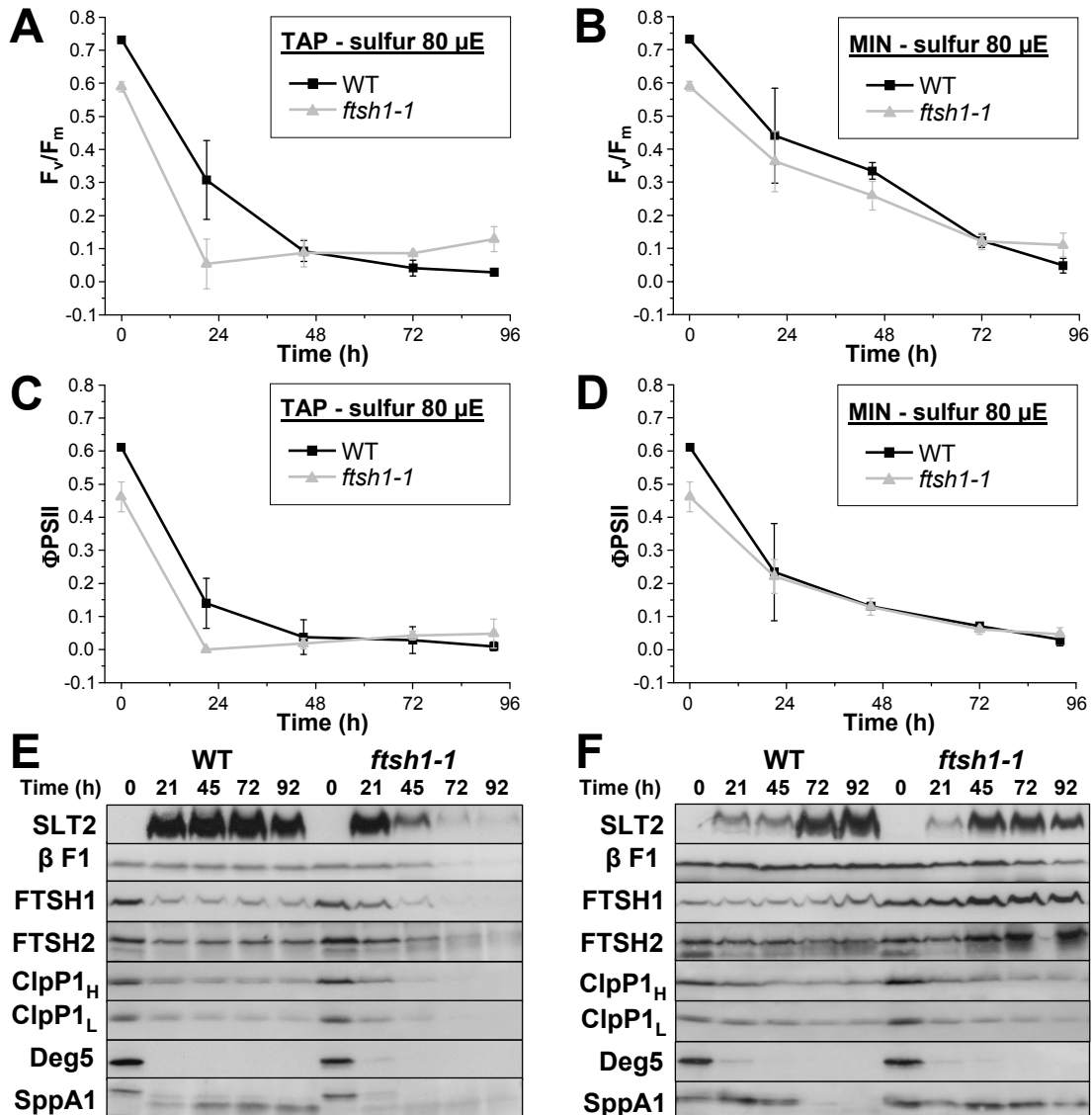
(B) Total cell proteins of vegetative diploids from cross *ftsh1-1 ccb2 arg7* X *FTSH1 ccb2 arg2* separated by SDS/urea-PAGE and analyzed by immunodetection with antibodies against cytochrome *b₆f* subunits show a low *b₆f* complex accumulation as in the *ccb2* mutant (Figure 2A).

(C) Vegetative diploids from *ftsh1-1 ccb2 arg7* X *FTSH1 ccb2 arg2* show a *b₆f* deficiency in fluorescence induction kinetics as the *ccb2* mutant (Figure 2B).



Supplemental Figure 6. PSII subunit D1 did not co-immunoprecipitate with the antibody against FtsH1 peptide.

Digitonin-solubilized membranes from wild-type and *ftsh1-1* strains were incubated with protein A-sepharose beads coupled to antibodies against a peptide of FtsH1 (α -FtsH1) or preimmune serum (pi). Aliquots of digitonin-solubilized membranes (sol) and immunoprecipitates (IP) were separated by SDS-PAGE on a 8% polyacrylamide gel in the presence of 8 M urea and analyzed by immunodetection with antibodies against FtsH1, FtsH2 and D1.



Supplemental Figure 7. Cell Response is Delayed and Thylakoid Proteases are Preserved upon Sulfur Starvation when Cell Viability Solely Depends on Photosynthesis.

(A) Time course of sulfur starvation in the presence of acetate under $80 \mu\text{E m}^{-2} \text{s}^{-1}$ in wild-type and *ftsh1-1* strains as monitored by PSII activity (F_v/F_m).

(B) Time course of sulfur starvation in the absence of acetate under $80 \mu\text{E m}^{-2} \text{s}^{-1}$ as monitored by PSII activity detection.

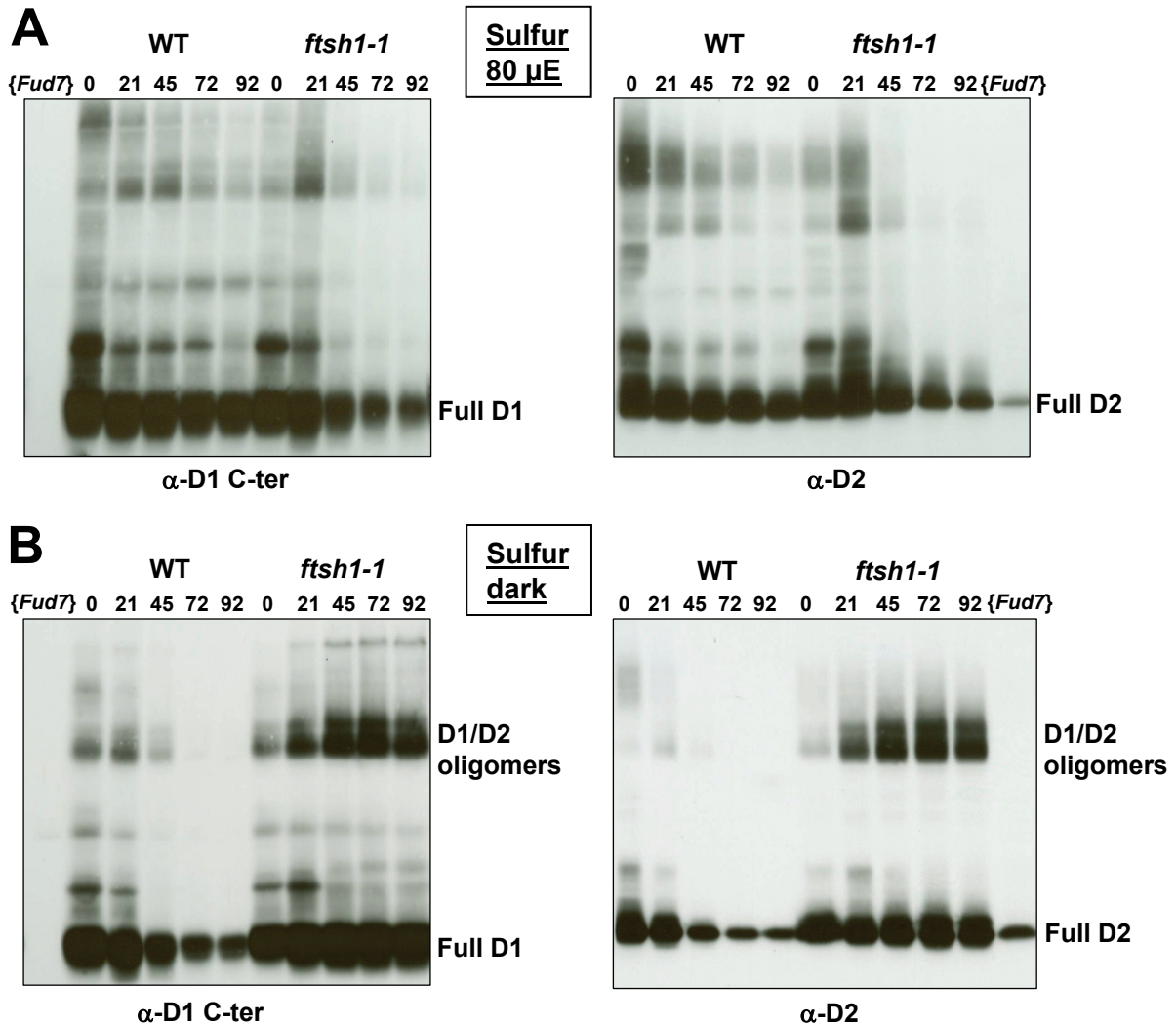
(C) Time course of sulfur starvation in the presence of acetate under $80 \mu\text{E m}^{-2} \text{s}^{-1}$ as monitored by downstream electron transfer (Φ_{PSII}).

(D) Time course of sulfur starvation in the absence of acetate under $80 \mu\text{E m}^{-2} \text{s}^{-1}$ as monitored by downstream electron transfer detection.

(E) Time course upon sulfur starvation in the presence of acetate under $80 \mu\text{E m}^{-2} \text{s}^{-1}$ as monitored by immunodetection of chloroplast proteases of the thylakoid (FtsH1, FtsH2, SppA1), stroma (unprocessed ClpP1_H and processed ClpP1_L) and lumen (Deg5), a marker of the cell response to sulfur deprivation (SLT2) and loading control ATP synthase β subunit (β F1). Total cell proteins were separated by SDS/urea-PAGE.

(F) Time course upon sulfur starvation in the absence of acetate under $80 \mu\text{E m}^{-2} \text{s}^{-1}$ as monitored by immunodetection.

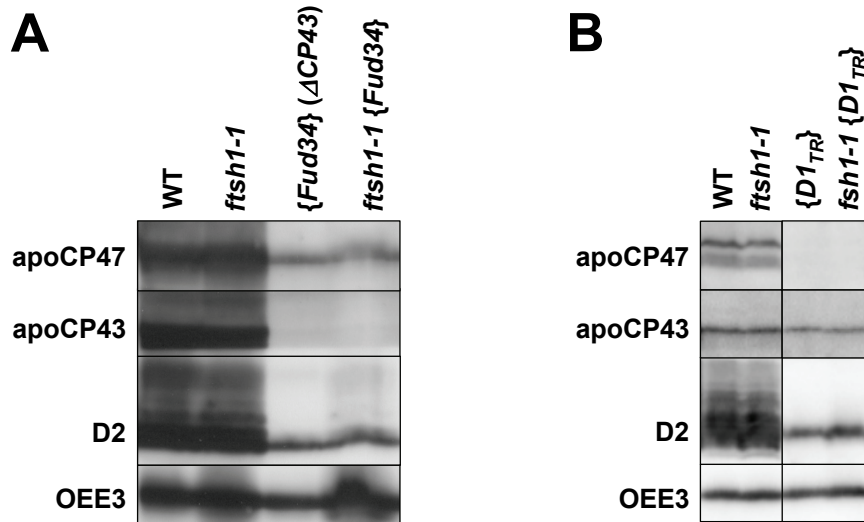
Means and standard deviations of two independent experiments for each starvation condition are given.



Supplemental Figure 8. D1/D2 Oligomers Accumulate Only in *ftsh1-1* Mutant upon Sulfur Starvation in the Dark.

(A) Time course of sulfur starvation under 80 μ E $m^{-2} s^{-1}$ in wild-type and *ftsh1-1* strains as monitored by immunodetection of PSII subunits D1 and D2 and their oligomers. The {*Fud7*} mutant containing a deletion in the chloroplast *psbA* gene which encodes D1 protein is used as a negative D1 control. Total cell proteins were separated on a denaturing 7.5-15% polyacrylamide gel in the presence of 8 M urea.

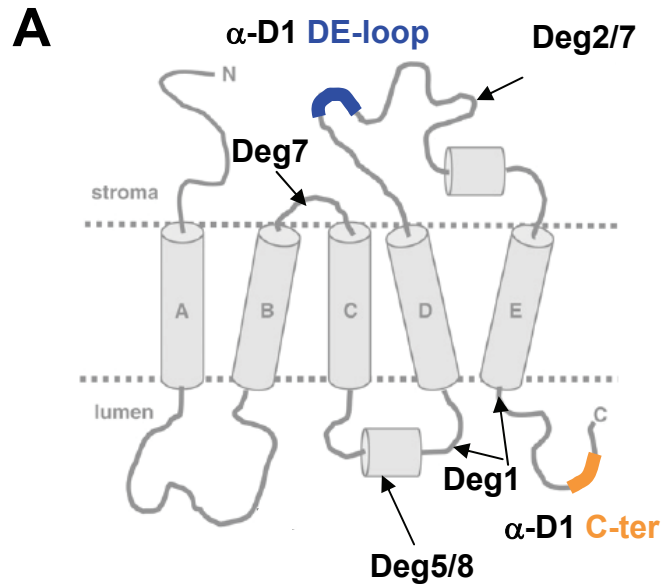
(B) Time course of sulfur starvation in the dark.



Supplemental Figure 9. *ftsh1-1* Does not Increase Accumulation of PSII Integral Subunits Lacking Assembly Partners.

(A) No overaccumulation of D2 or apoCP47 when apoCP43 is missing *{Fud34}* in *ftsh1-1* context. Total cell proteins were separated on a 12-18% polyacrylamide gel and analyzed by immunodetection.

(B) Not more of D2, CP47 or CP43 when D1 is truncated *{D1_{TR}}* in *ftsh1-1* context; total cell proteins were separated on a 16 % polyacrylamide gel and analyzed by immunodetection.



B

D1 fragments probed with α -D1 DE-loop

~ 23 kDa Deg2/7 cleavage in DE loop

D1 fragments probed with α -D1 C-ter

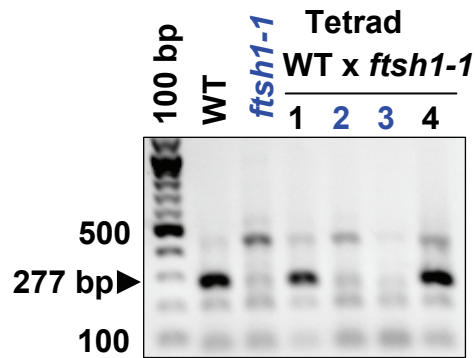
~16 kDa Deg7 cleavage in BC loop
 Deg5/8 cleavage in CD loop
 Deg1 cleavage in CD loop

~ 6 kDa Deg2/7 cleavage in DE loop
 Deg1 cleavage after TMH E

Supplemental Figure 10. D1 Fragments.

(A) D1 model (adapted from (Kapri-Pardes et al., 2007)) with the localization of Deg cleavage sites from *Arabidopsis* studies (Kapri-Pardes et al., 2007; Kato and Sakamoto, 2009; Kato et al., 2012; Sun et al., 2010) and localization of the D1 DE-loop and C-ter peptides.

(B) Obtained D1 fragments in *Chlamydomonas* detected with D1 DE-loop and C-ter antibodies and corresponding fragments predicted by the *Arabidopsis* model.



Supplemental Figure 11. PCR Test Used to Discriminate Between *ftsh1-1* and Wild-Type *FTSH1* alleles.

The wild-type genomic DNA *FTSH1* allele is specifically amplified with FtsH1-WTS and FtsH1-A3 primers as a 277 bp product. PCR products of wild-type, *ftsh1-1* and a tetrad progeny from a wild-type and *ftsh1-1* cross were separated on a 1% agarose gel together with a 100 bp DNA ladder.